1 February 1822 Compared to 1700-1850

The aim of the first task is to familiarize yourself with the CLIMEAPP and the reanalysis products of the PALEO-RA project. For this purpose, we examine the average temperature in February 1822 in relation to the reference period 1700-1850 (year-round). For that we utilize ModE-RA (use ModE-Sim and ModE-RAclim as well and note the differences!). Figure 1 presents a map-shaped global overview with temperature anomalies. An anomaly of up to +10°C can be observed over Scandinavia, extending across Siberia to eastern Russia. This anomaly gradually weakens towards southern Europe and eventually dissipates. Negative anomalies are evident over North America (south-eastern USA -0.5°C), Greenland (-4°C), Africa, and Central Asia (-2°C).

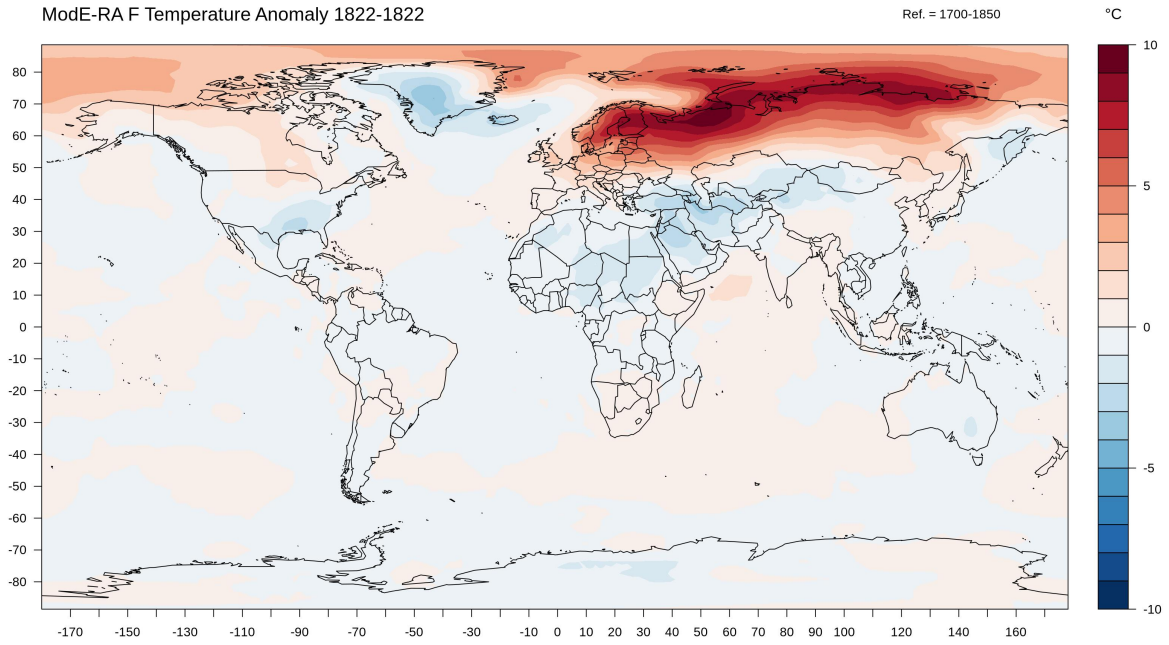

Figure 1: ModE-RA: Map of temperature anomaly of February 1822 compared to the 1700-1850 reference period.

2 Anomalies During Volcanic Years

As this solution serves only as an example, we focus exclusively on the volcanic years 1453 (an unidentified volcanic event evidenced by sulfur traces in ice cores, see: Sigl et al. 2013]) and 1815 (Tambora eruption). Our analysis focuses on temperature and precipitation anomalies and on the different products of the PALEO-RA project (a simulation (ModE-Sim) and two reanalyses (ModE-RA and ModE-RAclim)). ModE-Sim, a simulation without corrections based on observations but including volcanic forcing, is expected to have deviations compared to ModE-RA, which includes corrections based on observations. If there are no observations available, ModE-RA is identical to ModE-Sim. ModE-RAclim, where volcanic forcing has been averaged out but the volcanic signal is still included in the assimilated data, provides another perspective. To analyze other volcanic years, please follow the same procedure.

During a volcanic eruption, large amounts of sulfur dioxide are released, which eventually oxidize into sulfate aerosols. This process increases atmospheric optical depth (AOD) and thus scattering as well, leading to summer cooling (see: Robock et al. 2000). Further, we also can expect a reduction of the African Summer Monsoon due to inhomogeneous cooling of the land and ocean, which decreases the temperature gradient between Europe and Asia and the Pacific and Indian Oceans (see: Zambri et al. 2017).

2.1 Temperature Anomalies

ModE-RA shows a noticeable summer cooling during boreal summer for the unknown eruption in 1453 and especially for the Tambora eruption in 1815 (Fig. 4 and 5). Regarding the 1453 eruption, ModE-Sim depicts a positive anomaly over southeast Europe of about +0.5°C (Fig. 2), while ModE-RA displays a negative anomaly of about -0.5°C (Fig. 4). This discrepancy arises from corrections based on observations, where observations mainly consist of natural proxies like tree rings. If there is no observation available, ModE-Sim and ModE-RA are identically (hint: take a closer look to Africa and South America). ModE-RAclim also exhibits a boreal summer cooling (Fig. 6).

Figure 5 illustrates the Tambora eruption in 1815 generated by ModE-RA. The pronounced negative anomaly of about -2°C is notable (often referred to as the 'year without summer'). There is also a disparity between ModE-Sim (Fig. 3) and ModE-RA due to corrections based on observations (hint: take a closer look at Africa and South America again and note the change compared to 1453). ModE-RAclim exhibits a similar pattern to ModE-RA (Fig. 7).

2.2 Precipitation Anomalies

To investigate the precipitation anomaly over Africa, we essentially follow the same procedure as for the temperature anomaly. We observe that ModE-Sim (Fig. 8) and ModE-RA (Fig. 10) are identical for the year 1453 and show the same precipitation anomaly. This indicates that no observations were observable, and therefore, no corrections have been made. In 1815, however, we observe a difference between ModE-Sim (Fig. 9) and ModE-RA (Fig. 11), suggesting corrections based on observations. In both volcanic years, we observe a negative precipitation anomaly over central Africa, attributed to a reduction in the summer monsoon. Figures 12 and 13 show the anomaly using ModE-RAclim.

2.3 Plots: Temperature Anomaly

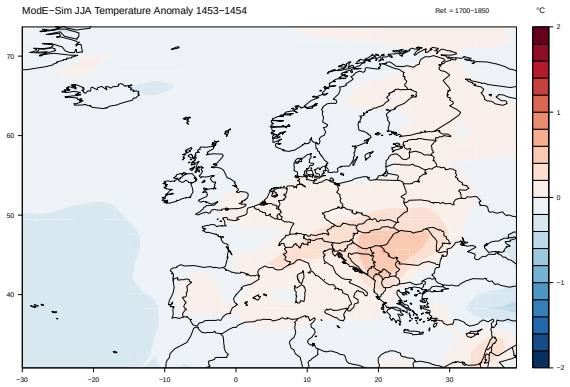

Figure 2: ModE-Sim: Map of temperature anomaly for the JJA Period of the year 1453 (unknown eruption) compared to the 1700-1850 reference period.

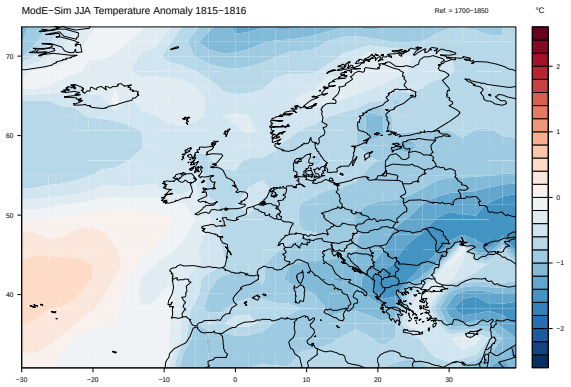

Figure 3: ModE-Sim: Map of temperature anomaly for the JJA Period of the year 1815 (Tambora eruption) compared to the 1700-1850 reference period.

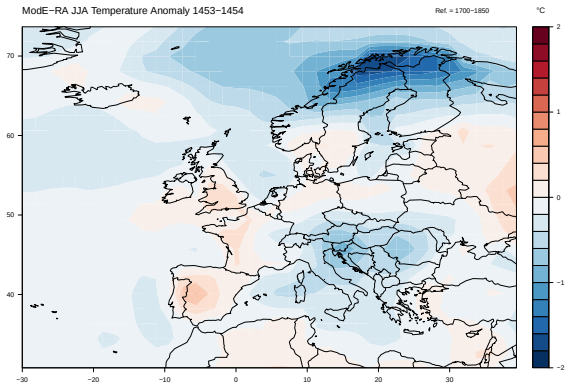

Figure 4: ModE-RA: Map of temperature anomaly for the JJA Period of the year 1453 (unknown eruption) compared to the 1700-1850 reference period.

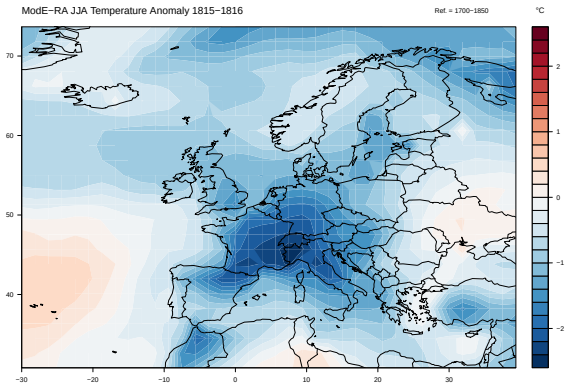

Figure 5: ModE-RA: Map of temperature anomaly for the JJA Period of the year 1815 (Tambora eruption) compared to the 1700-1850 reference period.

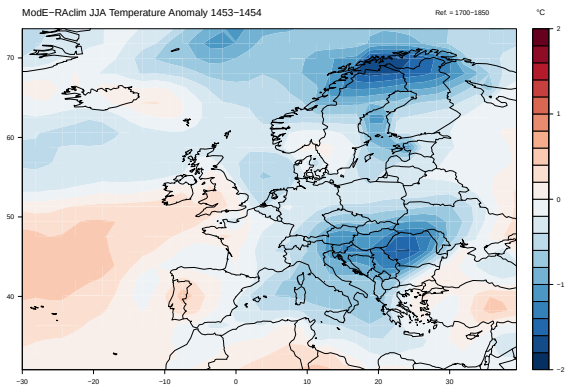

Figure 6: ModE-RAclim: Map of temperature anomaly for the JJA Period of the year 1453 (unknown eruption) compared to the 1700-1850 reference period.

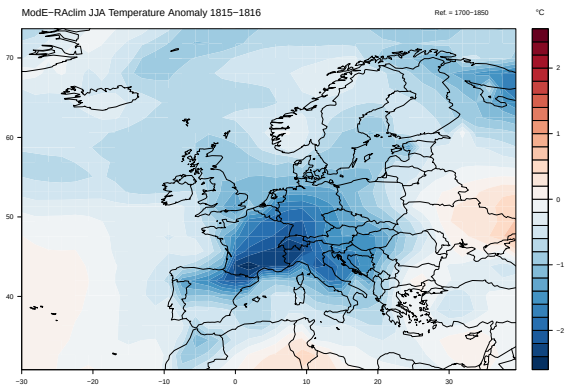

Figure 7: ModE-RA-clim: Map of temperature anomaly for the JJA Period of the year 1815 (Tambora eruption)) compared to the 1700-1850 reference period.

2.4 Plots: Precipitation Anomaly

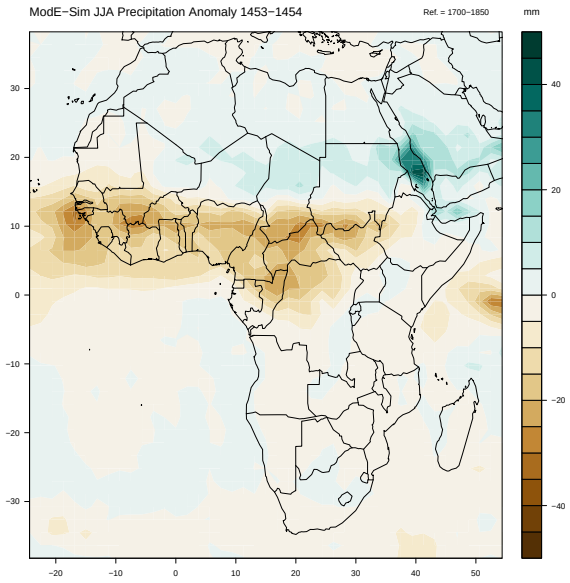

Figure 8: ModE-Sim: Map of precipitation anomaly for the JJA Period of the year 1453 (unknown eruption) compared to the 1700-1850 reference period.

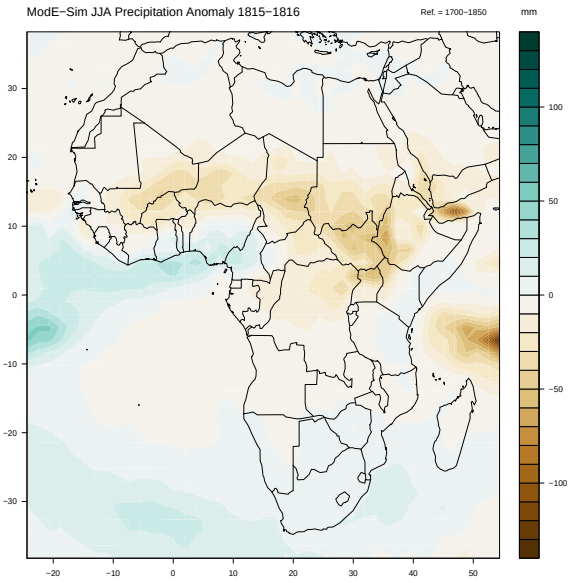

Figure 9: ModE-Sim: Map of precipitation anomaly for the JJA Period of the year 1815 (Tambora eruption) compared to the 1700-1850 reference period.

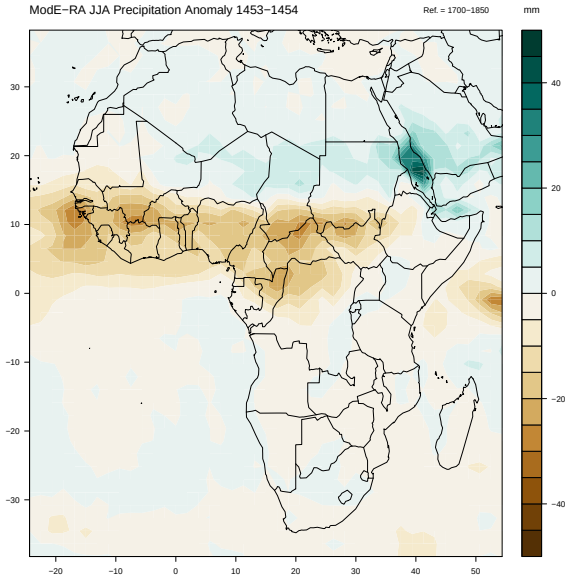

Figure 10: ModE-RA: Map of precipitation anomaly for the JJA Period of the year 1453 (unknown eruption) compared to the 1700-1850 reference period.

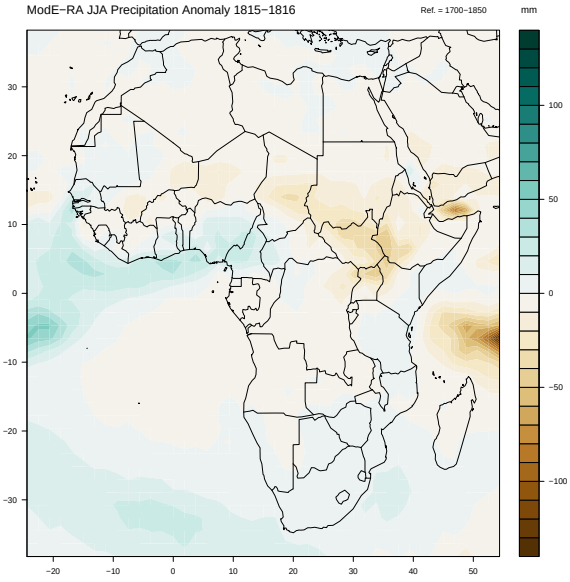

Figure 11: ModE-RA: Map of precipitation anomaly of the JJA Period for the year 1815 (Tambora eruption) compared to the 1700-1850 reference period.

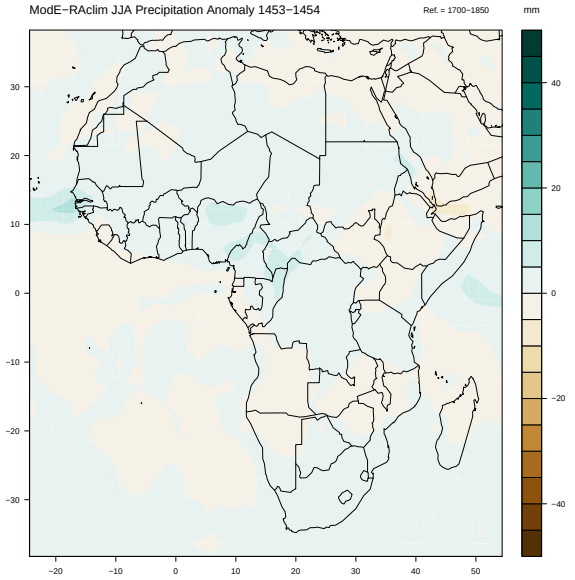

Figure 12: ModE-RAclim: Map of precipitation anomaly of the JJA Period for the year 1453 (unknown eruption) compared to the 1700-1850 reference period.

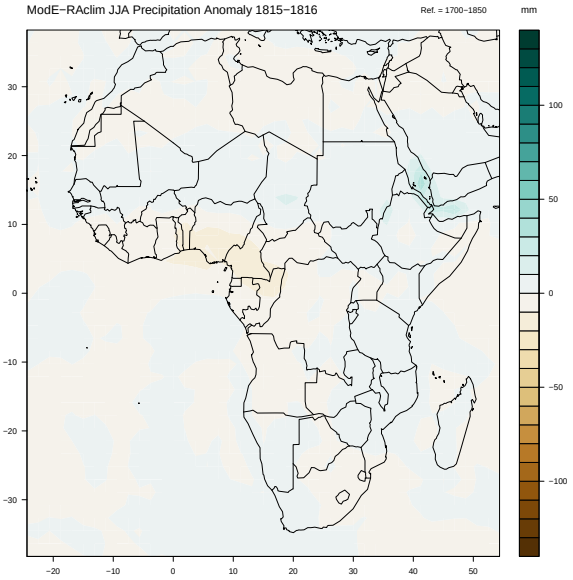

Figure 13: ModE-RAclim: Map of precipitation anomaly for the JJA period of the year 1815 (Tambora eruption) compared to the 1700-1850 reference period.

3 Regression

Here, we utilized the temperature in the Niño 3.4 index field and applied spatial linear regression on the global temperature between 1422 and 2008. Showing the regression coefficients, Figure 14 illustrates a typical El Niño pattern (a warmer central Pacific, positive anomaly over Canada and Australia, and cold in the southeast of the USA and Indonesia) and La Niña pattern (more or less vice versa to El Niño). For further information, refer to: Climatic Changes Since 1700, Brönnimann et al. 2015, p.113f.

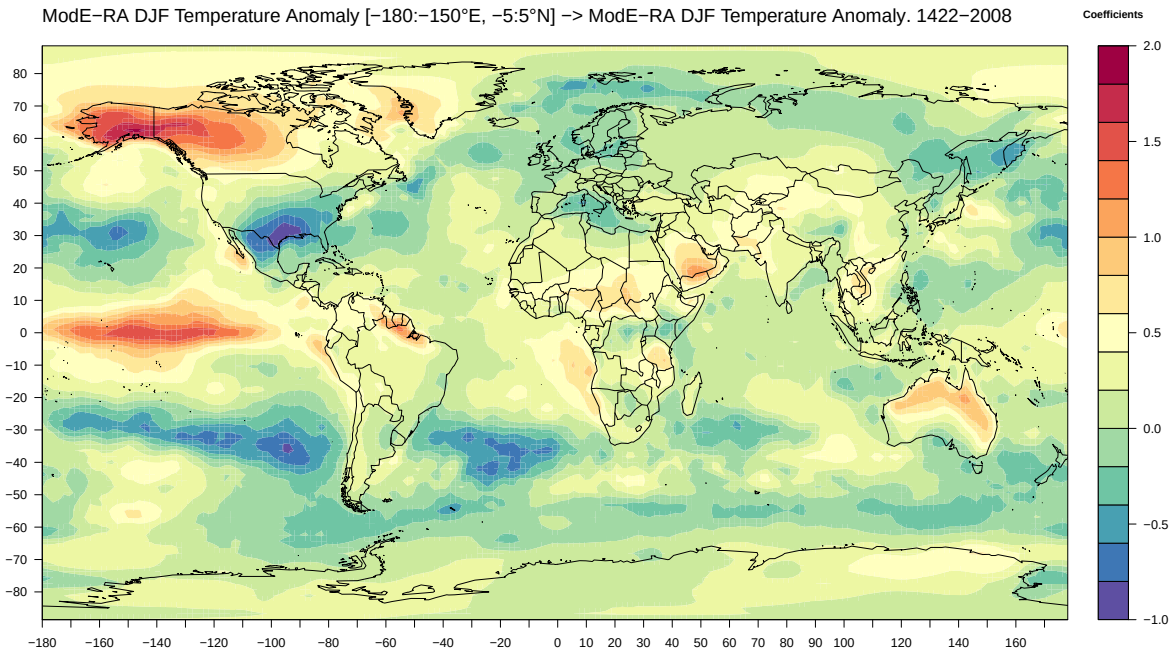

Figure 14: ModE-RA: Map of regression coefficients for the temperature of the Niño 3.4 index and the global temperature.